American Mineralogist, Volume 73, pages 714–726, 1988

Internally consistent solution models for Fe-Mg-Mn-Ti oxides: Fe-Ti oxides

DAVID J. ANDERSEN, DONALD H. LINDSLEY
Department of Earth and Space Sciences, State University of New York, Stony Brook, New York 11794-2100, U.S.A.

ABSTRACT

A model for coexisting ilmenite$_{ss}$-magnetite$_{ss}$ based on new and existing experimental data for the Fe-Ti oxides is developed using linear programming that is also internally consistent with the available data for Fe-Mg exchange for olivine$_{ss}$-ilmenite$_{ss}$ and olivine$_{ss}$-magnetite$_{ss}$ and Fe-Mn exchange for ilmenite$_{ss}$-garnet$_{ss}$. The model for ilmenite$_{ss}$ is based on a multicomponent Margules-type solution. For magnetite$_{ss}$, two models are developed: one based on an assumed Akimoto-type distribution for the cations and the other based on the available cation-distribution data for the binaries. Both spinel models are adequate in describing the macroscopic solution properties of magnetite-ulvöspinel solid solutions, and both predict an asymmetric miscibility gap below 500 °C.

INTRODUCTION

The magnetite$_{ss}$-ilmenite$_{ss}$ geothermometer and oxygen barometer calibrated by Buddington and Lindsley (1964; Lindsley, 1963) has been widely used since its introduction. Since then, numerous attempts have been made to model the exchange and oxidation reactions (Rumble, 1970; Powell and Powell, 1977; Spencer and Lindsley, 1981). The most recent formulation (Spencer and Lindsley, 1981) has been shown to give inconsistent results (Stormer, 1983); in addition, compositional departures from the system Fe-Ti-O have been treated in an empirical manner (e.g., Buddington and Lindsley, 1964; Anderson, 1968; Carmichael, 1967; Lindsley and Spencer, 1982; Stormer, 1983). The purpose of this study is to present new experimental data on the compositions of coexisting mt$_{ss}$-il$_{ss}$ (definitions and abbreviations are listed in Table 1), to revise the solution model for mt$_{ss}$ and il$_{ss}$ to include the effects of Mg and Mn, and to examine the effects of order-disorder on the solution properties of spinels. The calibrations presented here, which are based on an extended data base (Hammond et al., 1982; Lindsley and Podpora, 1983; Hadjigeorgiou et al., 1987; and this study), include the effects of Mg and Mn on mt$_{ss}$-il$_{ss}$ (Pinckney and Lindsley, 1976) and are consistent with (1) the Fe^{2+}-Mg exchange between olivine-and ilmenite (Andersen and Lindsley, 1979; 1981; Andersen, 1983; Bishop, 1976) and between olivine and spinel (Hill and Sack, 1987; Jamieson and Roedder, 1984) and (2) the Fe^{2+}-Mn^{2+} exchange between ilmenite and garnet (Kress, 1986). The new experiments were done in regions that, on the basis of initiated models, were ascertained to be critical areas of temperature and composition in modeling the solution parameters. Although this paper deals with the Fe-Ti oxides, treatment of the ilmenite-spinel-olivine-garnet data simultaneously (Andersen and Lindsley, in prep.), has yielded an internally consistent model.

Chemical equilibrium between mt$_{ss}$-il$_{ss}$ is described by the Fe-Ti exchange reaction

$$FeTiO_3 + Fe_3O_4 = Fe_2TiO_4 + Fe_2O_3,$$

where

$$\Delta G^0_{FeTi} = -RT \ln(a_{Usp}a_{Hem})/a_{Mt}a_{Il}), \tag{1}$$

and the oxidation reaction

$$4Fe_3O_4 + O_2 = 6Fe_2O_3, \tag{2}$$

where

$$\Delta G^0_{oxid} = -RT \ln[a^6_{Hem}/(a^4_{Mt}f_{O_2})]. \tag{3}$$

At low values of f_{O_2}, the stability of ulvöspinel is governed by

$$2FeTiO_3 + 2Fe + O_2 = 2Fe_2TiO_4$$

with

$$\Delta G^0_{ILIU} = -RT[a^2_{Fe_2TiO_4}/(a^2_{FeTiO_3}a^2_{Fe}f_{O_2})]. \tag{4}$$

Furthermore, the addition of fayalite to the system yields the reaction

$$\underset{qtz}{SiO_2} + \underset{usp}{2Fe_2TiO_4} = \underset{il}{2FeTiO_3} + \underset{fa}{Fe_2SiO_4},$$

where

$$\Delta g^0_{QUIIF} = RT \ln[a^2_{Il}a_{Fa}/(a^2_{Usp}a_{Qtz})]. \tag{5}$$

The term ΔG^0_r refers to the standard-state free-energy change for reaction r. Given values for the activities and the free energies of the end members, Equation 1 may be solved for temperature, and then given the temperature, Equation 3 for the f_{O_2} of the assemblage. However, the standard-state free energy for ulvöspinel is poorly known as are the activities of il$_{ss}$ and mt$_{ss}$. The mixing properties

0003–004X/88/0708–0714$02.00

of the two solid solutions can be derived from compositions of coexisting pairs at a known temperature and oxygen fugacity and a model for the activities of the components.

The free energy of a solid solution can be written as

$$G_{\text{total}} = G_{\text{end members}} - TS_{\text{conf}} + G_{\text{excess}}, \tag{6}$$

where S_{conf} is the configurational entropy and G_{excess} is an expression describing the excess energies of mixing. For molecular mixing, the configurational entropy can be written as

$$S_{\text{conf}} = -\alpha R \sum_i X_i \ln(X_i), \tag{7}$$

where X_i is the mole fraction of component i, and α is a constant related to the site multiplicity. For a multisite phase with random mixing of cations on each site, the configurational entropy can be written as (Thompson, 1969, 1970)

$$S_{\text{conf}} = -R \sum_s \sum_i b_s n_{i,s} \ln(n_{i,s}), \tag{8}$$

where b_s is the number of sites (s) per formula unit and $n_{i,s}$ is the fraction of n_i on site s. For mt_{ss} and il_{ss}, models for the configurational entropy will be developed using Equation 8, with various approximations to the site occupancies.

G_{excess} (Eq. 6) is modeled as a multicomponent asymmetric Margules (Wohl, 1946, 1953; Andersen and Lindsley, 1981) solution:

$$G_{\text{excess}} = \sum_i \sum_{j,j \neq i} W_{ij} X_i X_j \left(X_j + \sum_{k,k \neq i,j} X_k/2 \right) + \sum_i \sum_{j,j \neq i} \sum_{k,k \neq i,j} W_{ijk} X_i X_j X_k. \tag{9}$$

This differs from the expression used in Berman and Brown (1984) in that it includes an additional summation of $X_k/2$ in the coefficients for W_{ij}. Expressions for the activity coefficients derived from Equation 9 are then

$$\begin{aligned} RT \ln(\gamma_n) &= \sum_i \sum_{j,j \neq i} W_{ij} \Big\{ X_i X_j (X_j - X_i + 1) \\ &\quad - \sum_{m,m \neq n} X_m [Q_j (2X_j - X_i + 1) \\ &\quad + Q_i (X_j - 2X_i + 1)] \Big\} \\ &\quad + \sum_i \sum_{j,j \neq i} \sum_{k,k \neq i,j} W_{ijk} [X_i X_j X_k \\ &\quad - \sum_m X_m (Q_i X_j X_k + Q_j X_i X_k \\ &\quad + Q_k X_i X_j)], \end{aligned} \tag{10}$$

TABLE 1. Definitions and abbreviations

(A) =	site fraction of i on tetrahedral site, such that $\Sigma_i (A_i) = 1$
$[B]$ =	site fraction of j on octahedral site, such that $\Sigma_j [B_j] = 1$
a_i =	activity of component i
fa =	fayalite; Fa = Fe_2SiO_4
FMQ =	fayalite-magnetite-quartz buffer
f_{O_2} =	oxygen fugacity
G =	molar Gibbs energy
G_i^0 =	G of stoichiometric mineral i
G^* =	nonconfigurational or vibrational component of G
G^*_{0000}, G^*_{0010}, G^*_{1000} =	nonconfigurational or vibrational component of G for $(Fe^{2+})[Fe_2^{3+}]O_4$, $(Fe^{3+})[Fe^{2+}Fe^{3+}]O_4$, $(Fe^{2+})[Fe^{2+}Ti^{4+}]O_4$
g_i^*, g_{ij}^*, g_{ijk}^* =	coefficients of Taylor series expansion of g^*
hem =	hematite; Hem = Fe_2O_3 (h when subscript of Margules parameter)
iℓ =	ilmenite; iℓ = $FeTiO_3$ (i when subscript of Margules parameter)
$i\ell_{ss}$ =	R$\bar{3}$ ilmenites in the system $FeTiO_3$-Fe_2O_3
MH =	magnetite-hematite buffer
mt =	magnetite; Mt = Fe_3O_4
mt_{ss} =	spinel solid solution in the system Fe_3O_4-Fe_2TiO_4
N_i =	number of moles of chemical component i
QIF =	quartz-iron-fayalite buffer
qtz =	quartz; Qtz = SiO_2
R =	gas constant [8.3143 J/(mol·K)]
S_{conf} =	configurational entropy
T =	temperature (K)
usp =	ulvöspinel; Usp = Fe_2TiO_4
W_{ij} =	Margules-type terms to describe the nonideal mixing
X_i =	mole fraction of i
μ_i =	chemical potential of component i
μ_i^* =	vibrational component of the chemical potential
$\Delta\mu_{ij}^*$ =	difference in chemical potentials for exchange or reciprocal reactions

where Q_i is a term related to $\partial X_i/\partial X_m$ and

$$Q_i = 1 \ (m = i), \qquad -1 \ (i = n), \qquad 0 \ (m \neq i, \ i \neq n).$$

The temperature and pressure dependencies of the W terms are defined as

$$W = W_H - TW_S + (P - 1)W_V.$$

EXPERIMENTAL DETAILS

Starting materials consisted of mechanical mixes of prereacted phases (run conditions are listed in Table 2). For the 1-atm experiments, the mechanical mixes were loaded in $Ag_{80}Pd_{20}$ capsules in evacuated silica tubes, along with a capsule containing wüstite-magnetite buffer, and run in a vertical quench furnace. The 1- to 2-kbar experiments were loaded with 5 to 8 wt% H_2O into $Ag_{80}Pd_{20}$ capsules, sealed, and enclosed with hedenbergite-andradite-magnetite-quartz buffer plus H_2O in Au capsules. Standard hydrothermal cold-seal pressure vessels were used; the precision of the run temperature was estimated at ±5 °C, and the pressure varied less than ±50 bars. For the 5-kbar runs, the mechanical mixes were loaded into Fe-Pt capsules made from Pt tubing lined with one or two layers of Fe foil (0.0005 in. = 0.00127 cm) and annealed at 1200 °C for 1 to 2 d. The bulk composition of the capsule reported in Table 2 is based on the weight of the Pt tubing and Fe foil prior to annealing and assumes homogeneity. The annealing times were too short to produce a homogeneous capsule, but were sufficient to produce an inner wall consisting of an Fe-rich alloy, while the outer wall remained essentially pure Pt and thus helped maintain the in-

TABLE 2. Results of equilibration experiments for $i\ell_{ss}$-mt_{ss}

Run	T (°C)	P (kbar)	Duration (h)	Capsule	Initial	Final	X_{Fe} capsule	Buffer or flux
1	995	0	499	$Ag_{80}Pd_{20}$	$I\ell_{100}Usp_{80}$	$I\ell_{96.0}Usp_{80.5}$		WM
2	995	0	499	$Ag_{80}Pd_{20}$	$I\ell_{90}Usp_{90}$	$I\ell_{96.5}Usp_{81.0}$		WM
5	890	1	26	Au	$I\ell_{90}Usp_{20}$	$I\ell_{64.0}Usp_{25.0}$		HAMQ
6	890	1	11.5	Au	$I\ell_{70}Usp_{40}$	$I\ell_{62.0}Usp_{22.5}$		HAMQ
7	890	1	14.5	Au	$I\ell_{50}Usp_{30}$	$I\ell_{66.0}Usp_{26.0}$		HAMQ
8	800	2	107	Au	$I\ell_{70}Usp_{30}$	$I\ell_{76.5}Usp_{21.0}$		HAMQ
9	800	2	107	Au	$I\ell_{90}Usp_{10}$	$I\ell_{77.0}Usp_{20.0}$		HAMQ
12	1200	5	5	$Fe_{10}Pt_{90}$	$I\ell_{100}Usp_{80}$	$I\ell_{98.0}Usp_{93.5}$	0.48	5% $Na_2Si_2O_5$
13	1099	5	10.25	$Fe_{10}Pt_{90}$	$I\ell_{100}Usp_{80}$	$I\ell_{96.5}Usp_{91.5}$	0.45	5% $Na_2Si_2O_5$
14	1200	5	23	$Fe_{10}Pt_{90}$	$I\ell_{100}Usp_{80}$	$I\ell_{93.5}Usp_{78.5}$	0.36	5% $Na_2Si_2O_5$
15	1200	5	11.25	$Fe_{10}Pt_{90}$	$I\ell_{80}Usp_{95}$	$I\ell_{87.5}Usp_{75.0}$	0.31–0.32	5% $Na_2Si_2O_5$
16	1201	5	3.07	Fe_5Pt_{95}	$I\ell_{80}Usp_{96}$	$I\ell_{91.0}Usp_{78.5}$	0.33–0.34	5% $Na_2Si_2O_5$
17	1200	5	3.12	Fe_5Pt_{95}	$I\ell_{100}Usp_{70}$	$I\ell_{93.0}Usp_{84.0}$	0.36	5% $Na_2Si_2O_5$
18	1200	5	3.05	Fe_5Pt_{95}	$I\ell_{80}Usp_{95}$	$I\ell_{93.0}Usp_{84.5}$	0.38	5% $Na_2Si_2O_5$

Note: Compositions were determined from X-ray (1–9) and microprobe (12–18) with estimated uncertainties of ±1–2% and 0.5%, respectively. X_{Fe} is the composition of the "capsule" nearest the sample as determined by microprobe; the bulk composition is given under the heading "Capsule" (see text). WM and HAMQ are the wüstite-magnetite and hedenbergite-andradite-magnetite-quartz buffers.

tegrity of the capsule. These capsules were run in a piston-cylinder apparatus, using Pt-$Pt_{90}Rh_{10}$ thermocouples with the capsule located in the hot spot. The thermal gradient of the furnace assembly was known, and temperatures were adjusted accordingly. The precision of the reported temperature was estimated to be ±10 °C, and that of the nominal pressure, ±0.5 kbar, with no correction for the effect of pressure on the emf of the thermocouple.

Run products were examined using X-ray powder patterns, and compositions were determined using either X-ray curves or a CAMECA microprobe with ZAF corrections and the Fe^{3+} content calculated by assuming charge balance.

Ilmenite crystal chemistry

Pure hematite has the disordered $R\bar{3}c$ structure (Pauling and Hendricks, 1925), whereas pure ilmenite has the ordered $R\bar{3}$ structure (Barth and Posnjak, 1934) with distinct A and B layers and appears to retain this structure at least up to 1050 °C (Wechsler, 1978). At high temperatures, there is complete solid solution between ilmenite and hematite, implying that both have the same structure. However, only ilmenites close to $FeTiO_3$ in composition will be considered, and these should have crystallized in the ordered $R\bar{3}$ form. See Burton (1982) for a treatment of the $R\bar{3}c$-$R\bar{3}$ order-disorder transition in more Fe_2O_3-rich ilmenites, which will not be considered here.

The expression for the configurational entropy, S_{conf} (Eq. 8), assuming a random mixing of cations on each site, with the R^{2+} cations on the A site, Ti restricted to the B site, and Fe^{3+} mixing on both sites (Rumble, 1977), reduces to a molecular model with $\alpha = 2$ for Fe-Ti ilmenites. Expressions for the activities are then

$$RT\ln(a_{Il}) = 2RT\ln(X_{Il}) + 2X_{Il}X_{Hem}^2 W_{hi} + X_{Hem}^2(1 - 2X_{Il})W_{ih} \tag{11}$$

and

$$RT\ln(a_{Hem}) = 2RT\ln(X_{Hem}) + X_{Il}^2(1 - 2X_{Hem})W_{hi} + 2X_{Il}^2 X_{Hem} W_{ih},$$

where $X_{Il} + X_{Hem} = 1$.

Spinel crystal chemistry

The structure of spinels was recently reviewed by Lindsley (1976), Hill et al. (1979), and O'Neill and Navrotsky (1983, 1984), and only a brief description will be given here. The general formula is AB_2O_4, with the A and B cations having different valences. The unit cell (space group $Fd3m$) is face-centered cubic with 32 oxygens in nearly cubic-closest-packing. The cations fill the interstices within the oxygen framework, on 16 octahedral and 8 tetrahedral sites. A normal spinel has the single A cation in the tetrahedral site and the two B cations in the octahedral sites, written as $(A)[B_2]O_4$. Barth and Posnjak (1932) also suggested an alternative distribution with the B cation split between the octahedral and tetrahedral sites, $(B)[AB]O_4$, termed inverse by Verwey and Heilmann (1947).

Because of the importance of magnetite and ulvöspinel in understanding rock magnetism, a number of studies have been done to determine the cation distribution of Fe^{2+}-Fe^{3+} spinels. Both end-member magnetite and ulvöspinel have been considered to have the inverse distribution (see Wechsler et al., 1984), with Ti^{4+} restricted to the octahedral site, leading to the end members $(Fe^{3+})[Fe^{2+}Fe^{3+}]O_4$ and $(Fe^{2+})[Fe^{2+}Ti^{4+}]O_4$. For Fe_3O_4-Fe_2TiO_4 solutions, various models have been proposed to estimate the distribution of Fe^{2+} and Fe^{3+} in the solid-solution series.

Some support for the Akimoto model (Akimoto, 1954) comes from the recent work of Wechsler et al. (1984), who found no evidence of cation ordering, based on neutron-diffraction measurements of quenched samples. This model assumes that Ti^{4+} always replaces Fe^{3+} in the octahedral site, leading to the structural formula

$$(Fe_x^{2+}Fe_{1-x}^{3+})[Fe^{2+}Fe_{1-x}^{3+}Ti_x^{4+}]O_4, \qquad (0 \le x \le 1)$$

and assumes that magnetite retains the inverse structure at temperature. Jensen and Shive (1973) suggested that it is impossible to quench the high-temperature cation distribution, since it only requires the transfer of an electron between the two sites. Hence, measurements on quenched samples may not reflect the cation distribution at temperature. Stephenson (1969) and Bleil (1976) proposed a temperature-dependent ordering of Fe^{3+}, which approaches the Akimoto distribution at high temperature and the Néel-Chevallier (Néel, 1955; Chevallier et al., 1955) distribution at low temperatures.

Recent measurements of the variation of the Seebeck coefficient with temperature by Wu and Mason (1981) and Trestman-Matts et al. (1983) have shown that the octahedral valence ratio (=$[Fe^{2+}]/[Fe^{3+}]$) for mt_{ss} varies with temperature and composition. The site occupancies can then be calculated (Fig. 1) from composition and mass-balance constraints.

The importance of the site occupancies is in the calculation of the configurational entropy. Errors in the expression used for the S_{conf} are generally compensated by the ΔG_{excess} term; hence using a more nearly correct expression for S_{conf} should lead to simpler expressions for ΔG_{excess}.

Powell and Powell (1977) considered mt_{ss} to be ideal and used a molecular model for S_{conf} that leads to the following:

$$G_{end\ member} = \mu^0_{Usp}X_{Usp} + \mu^0_{Mt}X_{Mt}$$
$$S_{conf} = -R(X_{Usp}\ln X_{Usp} + X_{Mt}\ln X_{Mt})$$

and

$$G_{excess} = 0.$$

Spencer and Lindsley (1981) assumed that mt_{ss} is ideal above 800 °C and used an asymmetric binary Margules expression for G_{excess} below 800 °C,

$$G_{excess} = W_{Usp}X^2_{Mt}X_{Usp} + W_{Mt}X^2_{Usp}X_{Mt}. \tag{12}$$

Sack (1982), in a thermodynamic treatment of spinels in the system Fe-Mg-Al-Cr-Ti-O, wrote the free energy of $spinel_{ss}$ as

$$G = G^* - TS_{conf} \tag{13}$$

with

$$G^* = G_{ideal} + G_{excess}, \tag{14}$$

where G^*, the vibrational energy, includes both ideal and excess contributions to the free energy; Sack expanded G^* (Eq. 14) as a third-degree polynomial in terms of composition. Because of a limited amount of data, Sack (1982) was forced to make a number of simplifying assumptions. Because our knowledge of the cation distribution in Fe^{2+}-Fe^{3+}-Mg-Mn-Ti spinels is incomplete, especially for mixed compositions, as a first approximation, the same general form as that of Sack (1982) will be followed. As a second approximation, the effects of order-disorder on the configurational entropy will be considered.

Modified Akimoto model

As a first approximation we will consider that the spinels are perfectly inverse and the distribution of cations

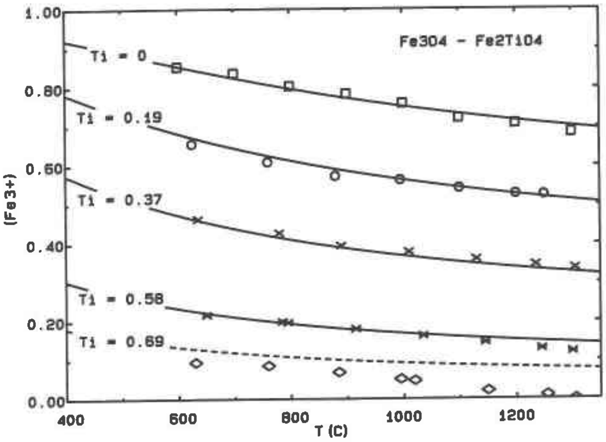

Fig. 1. $X_{(Fe^{3+})}$ vs. temperature for Fe_3O_4-Fe_2TiO_4 spinels at X_{Ti} = 0 (open squares), 0.19 (circles), 0.37 (x), 0.58 (*), and 0.69 (diamonds). The curves are calculated from the site-mixing model. As discussed in the text, the points at X_{Ti} = 0.69 were not used in the model. Data are from Wu and Mason (1981) and Trestman-Matts et al. (1983).

follows Akimoto's model; then the site occupancies may be calculated using the total site occupancy,

$$X_{(Fe^{2+})} + X_{(Fe^{3+})} = 1$$
$$X_{[Fe^{2+}]} + X_{[Fe^{3+}]} + X_{[Ti^{4+}]} = 1,$$

and mass-balance constraints,

$$N_{Fe^{2+}} = X_{(Fe^{2+})} + 2X_{[Fe^{2+}]} = 1 + X_2$$
$$N_{Fe^{3+}} = X_{(Fe^{3+})} + 2X_{[Fe^{3+}]} = 2 - 2X_2$$
$$N_{Ti^{4+}} = 2X_{[Ti^{4+}]} = X_2,$$

yielding

$$\begin{aligned} X_{(Fe^{2+})} &= X_2 \\ X_{(Fe^{3+})} &= (1 - X_2) \\ X_{[Fe^{2+}]} &= 1/2 \\ X_{[Fe^{3+}]} &= (1 - X_2)/2 \\ X_{[Ti^{4+}]} &= X_2/2. \end{aligned} \tag{15}$$

The vibrational energy, G^*, is expanded as a third-degree power series (Sack, 1982; Thompson, 1969, 1970) in terms of the independent compositional variable,

$$G^* = g^*_1 + g^*_2X_2 + g^*_{22}X^2_2 + g^*_{222}X^3_2.$$

The meanings of the individual g^*_{ijk} terms can be obtained by setting the compositions to the limiting end members and binaries (Thompson, 1969) and are listed in Table 3. For the Fe-Ti system this reduces to the same formulation used by Spencer and Lindsley (1981) but with $\alpha = 2$, $W_{12} = W_{Mt}$ and $W_{21} = W_{Usp}$. The vibrational energy, G^*, can then be rewritten in terms of the end-member energies and the excess terms,

$$G^* = G^*_{Fe_3O_4}(1 - X_2) + G^*_{Fe_2TiO_4}X_2 + W_{12}X^2_2(1 - X_2) + W_{21}X_2(1 - X_2)^2.$$

TABLE 3. Definition of G* in terms of end-member and excess energies for the modified Akimoto model

$g_1^* = G^*_{Fe_3O_4}$
$g_2^* = G^*_{Fe_2TiO_4} - G^*_{Fe_3O_4} + W_{21}$
$g_{22}^* = W_{12} - 2W_{21}$
$g_{222}^* = W_{21} - W_{12}$

The expression for S_{conf} (Eq. 8), combined with the definitions for the site occupancies (Eq. 15), reduces to

$$S_{conf} = -2R[X_2\ln(X_2) + (1 - X_2)\ln(1 - X_2) - \ln(2)].$$

Activity expressions can then be derived using Sack (1982) and Darken and Gurry (1953):

$$\mu_i = G + \sum_j (n_j - X_j)(\partial G/\partial X_j), \qquad (16)$$

where n_j is the number of moles of component j (from the linearly independent component, X_2). Since

$$\mu_i - \mu_i^0 = RT\ln(a_i), \qquad (17)$$

application of Equations 16 and 17 leads to the following activity expressions:

$$RT\ln(a_{Mt}) = 2RT\ln(1 - X_2) + X_2^2(2X_2 - 1)W_{12} + 2X_2^2(1 - X_2)W_{21} \qquad (18)$$

and

$$RT\ln(a_{Usp}) = 2RT\ln(X_2) + 2X_2(1 - X_2)^2W_{12} + (1 - 2X_2)(1 - X_2)^2W_{21}.$$

CALIBRATION OF THE AKIMOTO MODEL

From the expressions for the activities of mt_{ss} (Eq. 18), il_{ss} (Eq. 11), and the conditions for equilibrium for the exchange and oxidation reactions (Eqs. 1, 3), model parameters can be extracted from the experimental data on coexisting pairs of mt_{ss} and il_{ss}.

Compositions of coexisting mt_{ss} and il_{ss} for the system Fe-Ti-O were taken from Buddington and Lindsley (1964), Katsura et al. (1976), Spencer and Lindsley (1981), Hammond et al. (1982), Hadjigeorgiou et al. (1987), and Table 2. An uncertainty of ±3 mol% was applied to the data of Katsura et al. (1976). The data in Hammond et al. (1982) are somewhat contradictory and in the interest of internal consistency the points labeled "L" were used. The data of Taylor (1964) were excluded because of the uncertainty in stoichiometry of the phases. The data of Webster and Bright (1961) are inconsistent[1] with those of Katsura et al. (1976), and we have chosen to use the more recent set of data. The experiments listed in Table 2 using the HAMQ buffer and those in Fe-Pt capsules were treated as temperature constraints only (Eq. 1) because of uncertainties in the buffer calibration for HAMQ and the f_{O_2} imposed by the Fe-Pt capsules and oxide assemblage. Values for the appropriate buffers are from Haas (pers. comm.) and Chou (1978). The values from Haas (pers. comm.) were chosen because they are internally consistent and any errors in the calibrations should be systematic.

Additional constraints can be derived from the mt_{ss} miscibility gap; however, the location of the miscibility gap is uncertain because of the sluggish rates of reaction at low temperatures. The experiments by Vincent et al. (1957) were done on natural samples, and they suggested that the miscibility gap is asymmetric toward magnetite with a consolute point of 600 °C. Price (1981) used natural and synthetic samples in conjunction with a TEM study of the run products and suggested that the consolute point lies below 490 °C and the gap is nearly symmetric. Lindsley (1981), on the basis of experiments on synthetic samples suggested that the miscibility gap is similar to that of Vincent et al. (1957) and that the results of Price (1981) may reflect the effect of Mg. The results of Lindsley (1981), however, were based on "dissolving" experiments that do not unequivocally locate the miscibility gap. These experiments were used to constrain the model using the location of the spinodal curve, $\partial^2G/\partial X_2^2 > 0$.

The experimental data were fitted to the model by using linear programming instead of least squares for a variety of reasons. Linear programming has the advantage of testing whether the experimental data are consistent with the model. In addition, the exchange reaction is not independent of the oxidation reaction because the temperature derived from the exchange reaction is used to calculate the f_{O_2} of the assemblage. More important, in least-squares modeling there is the implied assumption that the distribution of errors around the constant vector is normally distributed, which is not the case for exchange experiments (unless, of course, equilibrium has been demonstrated by an overlapping reversal); instead it is some unknown function of the starting composition, reaction path, diffusion rate, and duration of the experiment.

Since linear programming generates an exact solution for a given objective function, estimated uncertainties of ±5° in experimental temperature and ±0.05–0.19 (based on uncertainties in the buffer calibrations) in the calculated f_{O_2} values [±10° and ±0.20 for the data of Katsura et al. (1976)] were included in the constraints. The best model was chosen in terms of the simplest activity models for mt_{ss} and il_{ss} that yielded a reasonable mt_{ss} miscibility gap and the calculated location of the stability of the assemblage quartz + ulvöspinel + ilmenite + fayalite in $T - f_{O_2}$ space. The best set of parameters[2] are listed in Table 4, and a revised $T - f_{O_2}$ diagram for the Fe-Ti system is shown in Figure 2. The oxygen fugacity is plotted relative to FMQ [$\Delta\log f_{O_2}$ (FMQ) $= \log_{10}f_{O_2} - \log_{10}f_{O_2}^{FMQ}$]

[1] Inconsistent, in the sense that for the activity models used here, both sets of experiments cannot be fit simultaneously.

[2] In the final model, the silica-tube experiments (Table 2 and those from Hammond et al., 1982) constrain only the exchange-reaction parameters. Although the actual values of oxygen fugacity in these experiments may be uncertain, that uncertainty does not affect the model because our preferred set of parameters is not constrained by the oxidation reaction for the silica-tube experiments.

TABLE 4. Model parameters [J/mol, J/(mol·K)]

	Preferred	Minimum	Maximum
ΔH_{FeTi}	2.9435300×10^4	2.661563×10^4	2.950790×10^4
ΔS_{FeTi}	4.5123500	2.218825	4.585932
		Ilmenite	
$W_{H,hi}$	4.4204800×10^4	3.916975×10^4	4.604088×10^4
$W_{S,hi}$	1.2274390×10	8.303420	1.399188×10
$W_{H,ih}$	1.2634250×10^5	1.073298×10^5	1.514754×10^5
$W_{S,ih}$	1.0060010×10^2	8.318893×10	1.199506×10^2
		Spinel (Akimoto distribution)	
$W_{H,12}$	1.5748030×10^4	1.489090×10^4	1.605777×10^4
$W_{H,21}$	4.6175480×10^4	2.652352×10^4	4.687425×10^4
$W_{S,21}$	2.3076500×10	5.670749	2.398282×10
		Spinel (site-mixing model)	
$\Delta\mu^*_{H,11}$	-2.023220×10^4	-2.023220×10^4	-2.023220×10^4
$\Delta\mu^*_{S,11}$	-1.094640×10	-1.094640×10	-1.094640×10
$W_{H,12}$	8.622861×10^2	-3.859675×10^3	1.465642×10^4
$W_{S,12}$	-2.353941×10	-2.741184×10	-1.247261×10
$W_{H,21}$	4.907650×10^4	2.944154×10^4	4.939171×10^4
$W_{S,21}$	3.167319×10	1.410198×10	3.176430×10
$W_{H,\bar{1}2}$†	-1.020241×10^4	-1.492438×10^4	3.591718×10^3
$W_{S,\bar{1}2}$†	-2.286705	-6.159142	8.780090
$W_{H,2\bar{1}}$†	3.801180×10^4	1.837684×10^4	3.832701×10^4
$W_{S,2\bar{1}}$†	5.292590×10	3.535468×10	5.301700×10
$W_{H,\bar{1}12}$†	4.821422×10^4	1.826445×10^4	5.295820×10^4
$W_{S,\bar{1}12}$†	5.521260×10	2.883191×10	5.883099×10
$W_{H,Fe}$	1.390470×10^4	7.769855×10^3	1.586290×10^4
$W_{S,Fe}$	2.531960×10	1.942474×10	2.700538×10

† Calculated from other W_H and W_S values.

because as noted by Frost and Myers (1982) this approach improves the readability of the graph though requires an additional calculation if absolute values of f_{O_2} are needed.

There are two types of uncertainties in the parameters in Table 4. The first is an assumed ±5° in T and ±0.05–0.19 log unit in f_{O_2}. The other is due to the width of the brackets. The preferred values listed in Table 4 are not unique, but it is not clear how to estimate the uncertainties to include the width of the experimental brackets. Minimum and maximum values for the model parameters are listed in Table 4, but since these values are correlated, they cannot be used to derive the uncertainties. In addition because the correlations are not ±1, the midpoints of the extreme values may not be a feasible solution. Selected isopleths calculated from the minimum and maximum solutions are drawn in Figure 3 and show the uncertainty in the location of the isopleths increasing at extreme values of T and f_{O_2}. These uncertainties might be larger than expected, but are due to the width of the compositional brackets and the uncertainty in T and f_{O_2} of the experiment. Note that the uncertainty bands are not symmetric abut the preferred model and become progressively wider outside the range of experimental data.

These values yield a mt_{ss} miscibility gap with a calculated consolute point of 491 °C and $X_2 = 0.344$; this is lower in temperature than estimated by Lindsley (1981) but is not inconsistent with those data and is more consistent with the data of Price (1981).

The stability of ulvöspinel at low values of f_{O_2} calculated using Eq. 4 and the QIF buffer of Haas (pers. comm.) is shown in Figure 2, along with experimentally determined values (Schmahl et al., 1960; Taylor and Schmalzreid, 1964; Webster and Bright, 1961; Taylor et al., 1972; Simons and Woermann, 1978) in Figure 4. The calculated curve is in broad agreement with the experimental data given that the accumulated uncertainty from

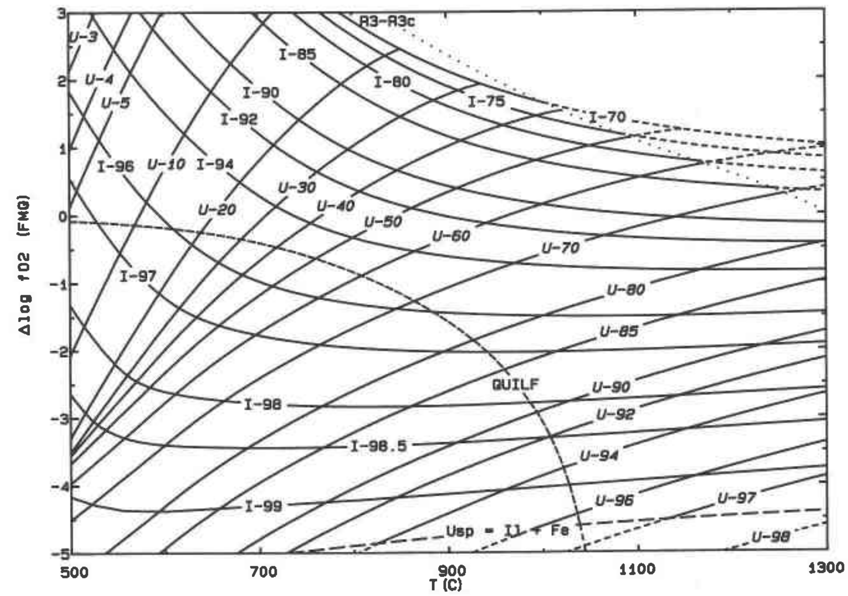

Fig. 2. Calculated isopleths of X_{Usp} and X_{Il} plotted as a function of $\Delta\log f_{O_2}$ (FMQ) versus temperature for the Akimoto distribution. The convergence of the X_{Usp} isopleths at low temperatures indicates the magnetite-ulvöspinel miscibility gap. The stability of the assemblages quartz + ulvöspinel + ilmenite + fayalite (QUIlF) and ulvöspinel + ilmenite + iron (usp = il + Fe) are also shown. The dotted line is the approximate location of the $R\bar{3}$-$R\bar{3}c$ transition for ilmenites (Burton, 1987).

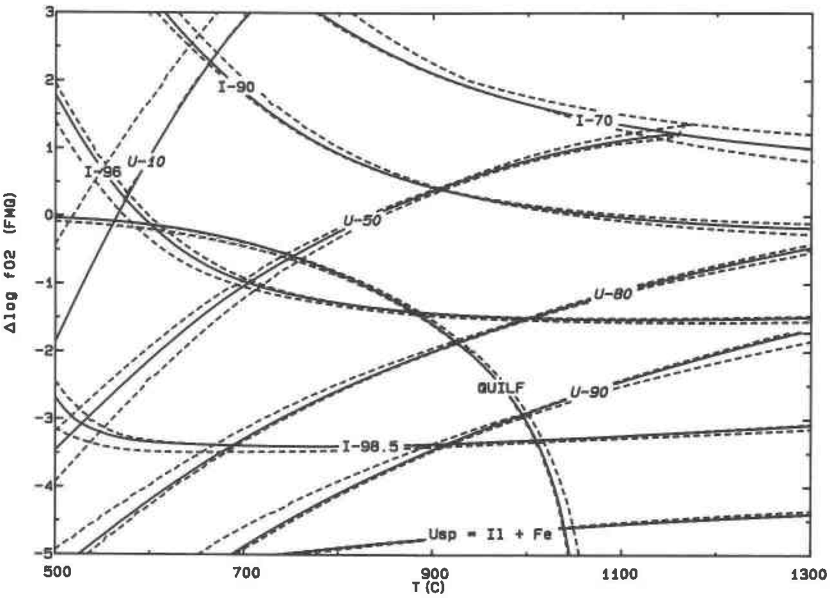

Fig. 3. Uncertainties in selected isopleths of X_{Usp} and X_{Il}, QUIlF, and usp = il + Fe for the Akimoto model. The solid lines correspond to the preferred solution parameters and the dashed lines are based on extreme values of the model parameters.

the buffer calibrations is ±0.05 log unit in f_{O_2} and that the calculation involves extrapolating the model to much lower f_{O_2} values than those at which it was calibrated.

The stability of the assemblage quartz + ulvöspinel + ilmenite + fayalite + Fe^0 in terms of temperature has been determined by El Goresy and Woermann (1977) at 1055 ± 5 °C and confirmed by Lindsley and Podpora (1983). At higher f_{O_2} values, the composition of mt_{ss} and il_{ss} is governed by the reaction,

$$SiO_2 + 2Fe_2TiO_4 = 2FeTiO_3 + Fe_2SiO_4(\text{QUIlF}). \quad (19)$$

The calculated location of this equilibrium (assuming $a_{SiO_2} = 1$ and $a_{Fe_2SiO_4} = 1$) intersects the curve for the stability of ulvöspinel and the QIF buffer at 1039 °C and $\Delta \log f_{O_2}$ (FMQ) = −4.60. This is slightly lower than the temperature of 1060 ± 3 °C determined by Lindsley and Podpora (1983). However, the calculated value is based on stoichiometric il_{ss} and mt_{ss}, and at this temperature, mt_{ss} in equilibrium with Fe is not stoichiometric (Simons and Woermann, 1981). For mt_{ss} and il_{ss}, this reaction is shown as a dashed line in Figure 2.

Uncertainty bands, based on minimum and maximum values of the model parameters, are shown in Figure 3 for these two reactions. Note that some solutions, although allowed by the experimental data, predict a higher upper-temperature limit for QUIlF (1052 °C) than the preferred model, but these solutions require a lower miscibility gap (350 °C) for mt_{ss}.

Spinel site mixing

The modified Akimoto model is adequate to explain the macroscopic properties of Fe-Ti spinels in equilibrium with ilmenite, but is based on an assumed cation distribution for the spinels that is inadequate given the recent work of Wu and Mason (1981) and Trestman-Matts et al. (1983). In this section, an alternative model for the mixing properties of spinels is developed, using the available cation-distribution data.

O'Neill and Navrotsky (1983, 1984) assumed that the enthalpy of disorder (ΔH_D) is proportional to the number of "wrong" cations on the tetrahedral site, with the standard state defined as the normal distribution,

$$\Delta H_D = X[\alpha + \beta X],$$

where α and β are constants and for mt_{ss}, X = fraction of Fe^{3+} on the tetrahedral site, and

$$\Delta G^0_{mix} = G_{cd,X} - XG_{X=1} - (1 - X)G_{X=0}$$

where cd = cation distribution and

$$\begin{aligned} \Delta G^0_{cd} &= \Delta H_D - T\Delta S_{conf} + \Delta G^0_{excess}, \\ \Delta G^0_{excess} &= WY(1 - Y), \\ Y &= Y_{Usp}, \end{aligned} \quad (20)$$

and the W (Eq. 20) is a term based on the size mismatch of the cations.

In a systematic study of spinels, O'Neill and Navrotsky (1983, 1984) found that the cation distribution of many binaries can be explained using this model. Trestman-Matts et al. (1983) found that the cation distribution for mt_{ss} is best explained using a temperature dependent β term and in order to fit the activity data of Katsura et al. (1975) for magnetite (calculated using the data of Webster and Bright, 1961, and Taylor, 1964), considered ΔG^0_{excess} to be of the form of an asymmetric binary Margules-type solution (Eq. 12).

With the assumption that Ti is restricted to the octahedral site (de Grave et al., 1975; Wechsler et al., 1984) and that Fe^{2+} and Fe^{3+} are disordered between the oc-

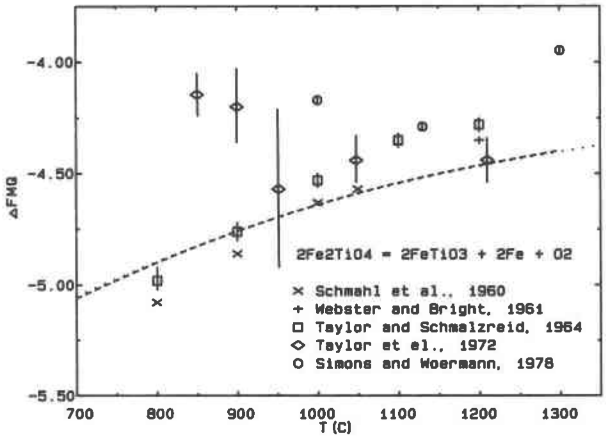

Fig. 4. The stability of ulvöspinel ($2Fe_2TiO_4 = 2FeTiO_3 + 2Fe^0 + O_2$) as a function of the $\Delta \log f_{O_2}$ (FMQ) values vs. temperature along with the experiments of Schmahl et al. (1960) (x), Webster and Bright (1961) (+), Taylor and Schmalzreid (1964) (squares), Taylor et al. (1972) (diamonds), and Simons and Woermann (1978) (circles). The dotted line is calculated from the Akimoto model; the dashed line for the site-mixing model. The two models are essentially the same for this reaction.

tahedral and tetrahedral sites but are randomly mixed on each (i.e., no short-range order), then the cation distribution can be described by adding one term to the expansion of G^* (Eq. 14), X_4, corresponding to the tetrahedral site occupancy of Fe^{3+}. The site occupancies, in terms of X_2 and X_4, can then be written in terms of the chosen components:

$$
\begin{aligned}
(Fe^{2+}) &= 1 - X_4 \\
(Fe^{3+}) &= X_4 \\
[Fe^{2+}] &= (1/2)(X_2 + X_4) \\
[Fe^{3+}] &= (1/2)(2 - 2X_2 - X_4) \\
[Ti^{4+}] &= (1/2)(X_2).
\end{aligned}
$$

Expansion of G^* as a third-degree Taylor series, treating Fe_3O_4-Fe_2TiO_4 as a ternary, with the components $(Fe^{2+})[Fe^{3+}Fe^{3+}]O_4$, $(Fe^{3+})[Fe^{2+}Fe^{3+}]O_4$, and (Fe^{2+})-$[Fe^{2+}Ti^{4+}]O_4$, and the definitions for G_{excess} of Andersen and Lindsley (1981), yields (meanings of the g^*_{ijk} terms are listed in Table 5)

$$
\begin{aligned}
G^* = {} & G^*_{0000}(1 - X_2) + G^*_{1000}X_2 + \Delta\mu^*_{\bar{1}1}X_4 \\
& + W_{\bar{1}1}X_4(1 - X_2 - X_4) \\
& + W_{12}X_2[X_4 - (1 - X_2)(1 - 2X_2)]/2 \\
& + W_{21}X_2[X_4 + (1 - X_2)(1 - 2X_2)]/2 \\
& + W_{Fe}X_2(1 - X_2 - X_4)
\end{aligned}
\tag{21}
$$

with

$$\Delta\mu^*_{\bar{1}1} = G^*_{0010} - G^*_{0000}$$

and

$$W_{Fe} = (W_{\bar{1}2} + W_{2\bar{1}})/2,$$

where the $(Fe^{2+})[Fe^{3+}Fe^{3+}]O_4 - (Fe^{3+})[Fe^{2+}Fe^{3+}]O_4$ join is treated as a symmetric binary ($W_{\bar{1}1}$), and the joins

TABLE 5. Definition of G^* in terms of end-member and excess energies for the model incorporating site mixing

$$
\begin{aligned}
g^*_1 &= G^*_{0000} \\
g^*_2 &= G^*_{1000} - G^*_{0000} + W_{Fe} + (W_{21} - W_{12})/2 \\
g^*_4 &= \Delta\mu^*_{\bar{1}1} + W_{\bar{1}1} \\
g^*_{22} &= -W_{Fe} - (3/2)(W_{21} - W_{12}) \\
g^*_{24} &= (W_{12} + W_{21})/2 - W_{Fe} - W_{\bar{1}1} \\
g^*_{44} &= -W_{\bar{1}1} \\
g^*_{222} &= W_{21} - W_{12}
\end{aligned}
$$

$$
\begin{aligned}
G^*_{0010} &= \Delta\mu^*_{\bar{1}1} + G^*_{0000} \\
W_{Fe} &= (W_{\bar{1}2} + W_{2\bar{1}})/2 \\
W_{\bar{1}2} &= W_{Fe} + (W_{12} - W_{21})/2 \\
W_{2\bar{1}} &= W_{Fe} - (W_{12} - W_{21})/2 \\
W_{\bar{1}12} &= W_{21} - W_{12}
\end{aligned}
$$

$(Fe^{2+})[Fe^{3+}Fe^{3+}]O_4$-$(Fe^{2+})[Fe^{2+}Ti^{4+}]O_4$ ($W_{\bar{1}2}$ and $W_{2\bar{1}}$) and $(Fe^{3+})[Fe^{2+}Fe^{3+}]O_4$-$(Fe^{2+})[Fe^{2+}Ti^{4+}]O_4$ (W_{12} and W_{21}) are treated as asymmetric binaries. Since the cation-distribution data for mt_{ss} do not justify more than a second-degree fit in terms of either X_2 and X_4, the terms g^*_{224}, g^*_{244}, and g^*_{444} have been set to zero. As a consequence of this, the ternary term $W_{\bar{1}12} = W_{21} - W_{12}$, and $W_{\bar{1}2}$ is not independent of $W_{2\bar{1}}$.

The terms in Eq. 21 can be divided into two groups, those describing energies for the end members and nonideal or excess terms. For the end members, one term is defined to describe the differences between the inverse and normal cation distributions for magnetite, $\Delta\mu^*_{\bar{1}1}$, and two terms for the end members, G^*_{0000} (normal magnetite), and G^*_{1000} (ulvöspinel). Because the standard-state energy is defined as that of the end member at the temperature and pressure of interest, these last two terms drop out of the activity expressions.

The excess terms can be further subdivided into excess energies arising from two types of interactions: mixing of cations between the octahedral and tetrahedral sites ($W_{\bar{1}1}$) and mixing of charge-coupled cations between the sites (W_{Fe}, W_{12}, and W_{21}). For mixing between 2-3 and 2-4 spinels, the inclusion of the third-degree terms allows for asymmetric excess energies of mixing between pairs of cations that are charge-coupled,

$$[Fe^{3+}Fe^{3+}] - [Fe^{2+}Ti^{4+}]$$

and

$$(Fe^{3+})[Fe^{3+}] - (Fe^{2+})[Ti^{4+}].$$

As in the previous section (Eq. 13)

$$G = G^* - TS_{conf}, \tag{22}$$

and the configurational entropy (Eq. 7) expands to

$$
\begin{aligned}
S_{conf} = -R[& 1 - X_4)\ln(1 - X_4) + X_4\ln(X_4) \\
& + (X_2 + X_4)\ln(X_2 + X_4) \\
& + (2 - 2X_2 - X_4)\ln(2 - 2X_2 - X_4) \\
& + X_2\ln(X_2) - 2\ln(2)].
\end{aligned}
\tag{23}
$$

Activity expressions can then be derived using Equation 16 where the standard state is defined as that of the pure component at the temperature and pressure of interest,

$$RT\ln(a_i) = \mu_i - \mu_i^0,$$

where μ_i and μ_i^0 are derived from Equation 17. Then

$$\begin{aligned} RT\ln(a_{Mt}) = {} & RT\ln[(1 - X_4)(2 - 2X_2 - X_4)^2] \\ & + W_{I1}X_4(X_2 + X_4) \\ & + X_4X_2[W_{Fe} - (W_{12} + W_{21})/2] \\ & + X_2^2[W_{Fe} + (1.5 - 2X_2)(W_{21} - W_{12})] \\ & - \{\ln[(1 - X_{4,Mt})(2 - X_{4,Mt})^2] \\ & \quad + W_{I1}X_{4,Mt}^2\} \end{aligned} \tag{24}$$

and

$$\begin{aligned} RT\ln(a_{Usp}) = {} & RT\ln[(1 - X_4)X_2(X_2 + X_4)] \\ & + W_{I1}X_4(X_4 - 1 + X_2) \\ & + X_4(1 - X_2)[(W_{12} + W_{21})/2 - W_{Fe}] \\ & + (W_{21} - W_{12})[1 - 6X_2 - X_2^2 \\ & \qquad \cdot(4X_2 - 9)]/2 \\ & + W_{Fe}(1 - X_2)^2, \end{aligned}$$

where $X_{4,Mt} = X_4$ for pure magnetite.

Calibration of the site-mixing model

For internal equilibrium the free energy of mt_{ss} is at a minimum with respect to the order parameter, X_4. The conditions for internal equilibria can then be derived from Equations 21 and 23 yielding

$$\begin{aligned} (\partial G/\partial X_4)_{X_2} & = 0 \\ & = RT\ln\{X_4(X_2 + X_4)/[(1 - X_4) \\ & \qquad \cdot(2 - 2X_2 - X_4)]\} \\ & \quad + \Delta\mu_{I1}^* + W_{I1}(1 - X_2 - 2X_4) \\ & \quad + X_2(W_{12} + W_{21})/2 \\ & \quad - W_{Fe}X_2. \end{aligned} \tag{25}$$

This reduces to the same form for $\partial G_{mix}/\partial X_4$ as that used by O'Neill and Navrotsky (1983, 1984), if $\alpha = \Delta\mu_{I1}^* + W_{I1}$, $\beta = W_{I1}$, and $W_{12} + W_{21} - 2W_{Fe} - W_{I1} = 0$. The mt_{ss} site-occupancy data can be fitted to this equation using a conventional least-squares approach. The Fe_3O_4-$MgFe_2O_{4,ss}$ data (Trestman-Matts et al., 1984), however, are nonlinear because only the octahedral Fe valence ratio is known. A modified version of the Simplex method (Nedler and Mead, 1965) was used to minimize

$$\sum_i (X_i - x_i)^2,$$

where X_i and x_i are the measured and calculated order parameters for data set i. The Fe_3O_4-Fe_2TiO_4 data at $X_2 = 0.69$ (Trestman-Matts et al., 1983) were not used in the fit because of the presence of a small amount of il_{ss} in the samples, which changes the bulk composition and biases the calculated site occupancies.[3]

The values for the preferred solution in terms of the minimum number of parameters are listed in Table 4, and calculated curves are shown in Figure 1. The terms $-W_{Fe} - (3/2)(W_{21} - W_{12})$ and $W_{21} - W_{12}$ are independent of the cation distribution and were derived from the mt_{ss}-il_{ss} data. Although this method does not give the uncertainties in the parameters, the overall error of the function can be estimated from the standard deviation of the residuals ($\sigma = 0.011$). The value for $\Delta\mu_{I1}^*$ is slightly different from that calculated by Wu and Mason (1981), but this gives a better fit to the mt_{ss} and magnetite–magnesium ferrite data (Andersen and Lindsley, in prep.).

As noted by Trestman-Matts et al. (1983), calculated cation distributions approach the Akimoto model at a temperature less than 500 °C, the Néel-Chevallier (Néel, 1955; Chevallier, 1955) model at very low temperatures, and the O'Reilly-Bannerjee (O'Reilly and Bannerjee, 1965) model at some intermediate temperature. This suggests that the cation distribution measured on quenched samples is dependent on the quench rate and may explain the variation in magnetic data noted by Wechsler et al. (1984).

The model for the site mixing was also included in the fit to the il_{ss}-mt_{ss} data, thus yielding one ilmenite model that is consistent with both spinel models. The parameters are listed in Table 4. The cation-distribution model, however, was derived separately. A calculated T-f_{O_2} diagram for the Fe-Ti system based on site mixing in spinels is shown in Figure 5, and estimates of the uncertainty of the isopleths are shown in Figure 6. Note that the uncertainties are not symmetric about the model values. This model predicts a mt_{ss} miscibility gap at 490 °C and $X_2 = 0.370$. This is at a similar temperature and is slightly more symmetric than that calculated from the previous model ($T = 491$ °C and $X_2 = 0.344$).

From the relations developed in the previous section (Eq. 19), the location of the stability of ulvöspinel and QUIlF is plotted in Figures 5 and 4. These are similar to the curves in Figure 2 and the curve in Figure 4 for the Akimoto model; the differences are minor. The intersection of QUIlF with the stability of ulvöspinel is also similar, 1040 °C and $\Delta\log f_{O_2}$ (FMQ) = −4.60.

Discussion

As can be seen from comparing Figures 2 and 5, the differences between the two spinel models are minor. This similarity reflects the facts that models that were chosen to yield temperatures for QUIlF at Fe saturation similar to the experimental data and the models predict similar miscibility gaps for mt_{ss}. The differences for coexisting mt_{ss}-il_{ss} are small in the range of the experimental data and become larger at extremes in T and f_{O_2}. Thus, to a good first approximation, the effects of cation ordering on the macroscopic properties of mt_{ss} can be neglected.

One uncertainty in the model is the effect of the $R\bar{3}$-$R\bar{3}c$ transition on the solution properties of the ilmenites. The value for ΔG^0_{oxid} in Equation 3 is from the MH buffer of Haas (pers. comm.) and implies a disordered $R\bar{3}c$ stan-

[3] Inclusion of this data set ($X_2 = 0.69$) worsens the fit and introduces systematic biases for the data at lower Ti contents ($X_2 < 0.69$); these difficulties may reflect the inadequacy of the formulism used here to describe the cation ordering for Ti-rich magnetites.

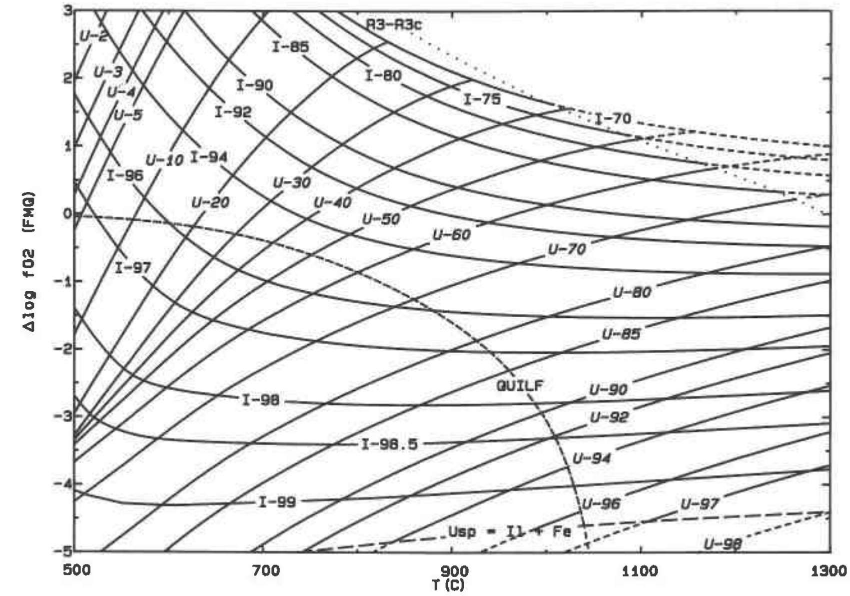

Fig. 5. Calculated isopleths of X_{Usp} and X_{Il} plotted as a function of the $\Delta \log f_{O_2}$ (FMQ) values vs. temperature for the site-mixing model. Compare to Figure 2 at low temperatures. The stabilities of the assemblages of QUIlF and usp = il + Fe are also shown, as is the approximate location of the $R\bar{3}$-$R\bar{3}c$ transition for il_{ss} (Burton, 1987).

dard state for hematite. Models incorporating a simple $\Delta H_{R\bar{3}\text{-}R\bar{3}c}$ correction did not improve the fit, although small values are consistent with the data. Any effects of this transition on the solution properties must be implicitly incorporated in the solution parameters.

The differences between the two models for the mixing properties of the spinels are shown in Figure 7, where calculated values for

$$\Delta G_{mix} = G_{solution} - (1 - X_2)G_{Mt} - X_2 G_{Usp}$$
$$\Delta S_{mix} = T(S_{conf,solution} - (1 - X_2)S_{conf,Mt} - X_2 S_{conf,Usp})$$
$$\Delta G_{excess} = \Delta G_{mix} - \Delta S_{mix}$$

are plotted at 400 °C (Fig. 7a) and 1200 °C (Fig. 7b). The similarity for ΔG_{mix} for both models reflects the relatively tight constraints imposed by the experimental data and

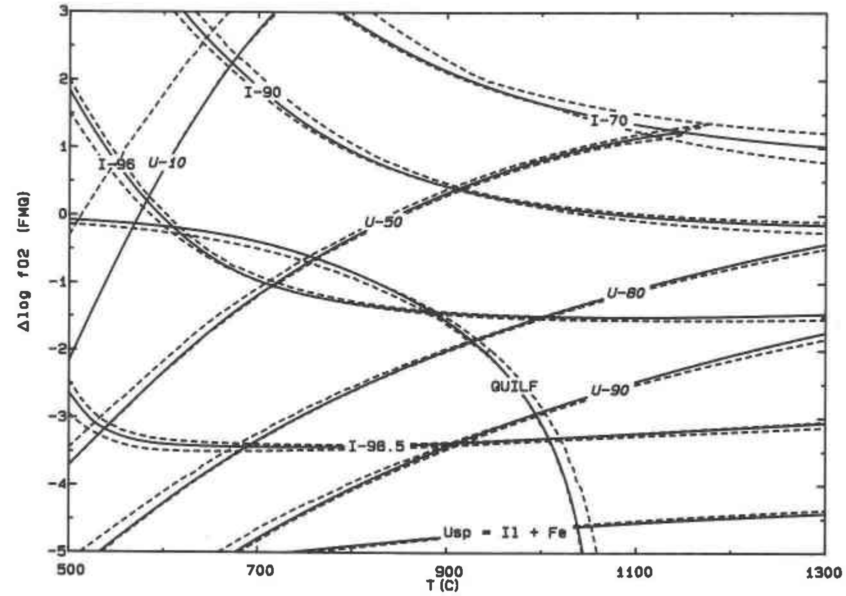

Fig. 6. Uncertainties in selected isopleths of X_{Usp} and X_{Il}, QUIlF, and usp = il + Fe for the site-mixing model based on the extreme values of the model parameters (symbols as in Fig. 3).

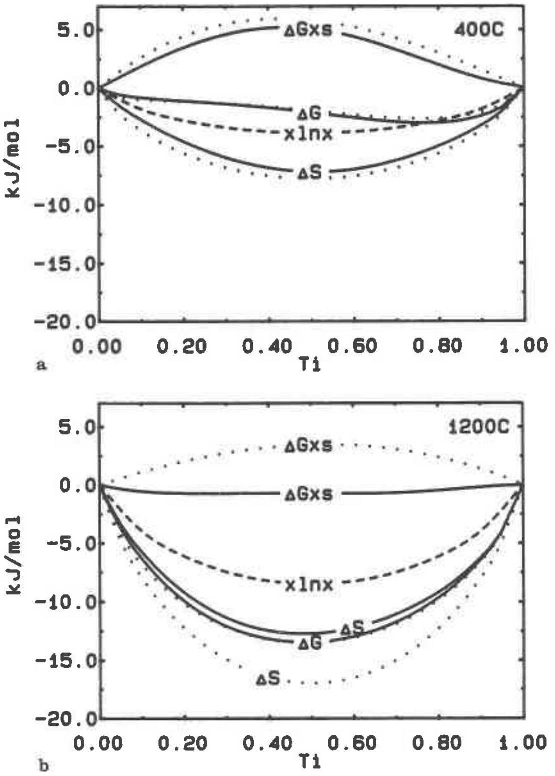

Fig. 7. Calculated values for ΔG_{mix}, ΔS_{mix}, ΔG_{excess} vs. X_{Ti} at 400 °C (**a**) and 1200 °C (**b**) for the Akimoto distribution (dotted line) and site-mixing model (solid lines). The curve labeled x ln x is ΔS_{mix} for a molecular model.

the fact that both models were constrained to the same ilmenite solution. Since the cation distribution in spinels approaches the Akimoto distribution at low temperatures, ΔS_{mix} and ΔG_{excess} are similar for both models at 400 °C. At 1200 °C, ΔG_{mix} for the site-mixing model is dominated by the ΔS_{mix} term, and ΔG_{excess} is slightly negative, whereas ΔG_{excess} for the Akimoto model requires positive values. A molecular model (α = 1 in Eq. 8), implying short-range order, for ΔS_{mix} (labeled x ln x in Fig. 7) would seem to require smaller values for ΔG_{excess} at low temperatures, for the same values of ΔG_{mix} for both mt_{ss} and il_{ss}. This may be reflecting the "hint" of short-range order suggested by the cation-distribution data of Wechsler et al. (1984) for quenched samples of mt_{ss}.

Conclusions

An internally consistent model for il_{ss}-mt_{ss} has been developed that should be an improvement over previous calibrations because the models are consistent with all of the chosen experimental data and the effects of Mg and Mn have been explicitly included (Andersen and Lindsley, in prep.). Differences between T and f_{O_2} values calculated from these models and those of previous calibrations (e.g., Buddington and Lindsley, 1964; Spencer and Lindsley, 1981) are primarily due to the more recent buffer calibrations, an extended data set, and extrapolating the previous models outside of the range of calibration. Application of current models to natural samples outside the range of the experimental calibration will lead to larger uncertainties than shown in Figures 3 and 6 because the functional form of the model is also being extrapolated. In addition, any nonstoichiometry that may be present in either mt_{ss} or il_{ss} has not been accounted for.

In terms of the system Fe-Ti-O, between 600 and 1200 °C and oxygen fugacities between the NNO and WM buffers, there is little difference between the two models, in calculated temperatures and oxygen fugacities. The major differences between the two models occur with extrapolating the models to lower and higher temperatures [compare Figs. 2 and 5 at 500 °C and at 1300 °C, most noticeably at 500 °C and high values of $\Delta \log f_{O_2}$ (FMQ), where small changes in the ulvöspinel content of mt_{ss} lead to relatively large differences in f_{O_2}].

Since both models for the spinels are adequate to describe the macroscopic properties of the spinels, within the range of experimental data, the Akimoto model might be preferred because the calculation of T and f_{O_2} is simpler.

Programs to calculate T and f_{O_2} for coexisting oxides are available from the authors.

Acknowledgments

We thank Ron Frost, Ben Burton, Paula Davidson, and Khal Spencer for helpful discussions, Carol Nabelek and Anita Grunder for probing some of the experiments, John Haas for providing unpublished values for the oxygen buffers, R. O. Sack and B. J. Wood for perceptive reviews and the National Science Foundation (grants EAR 8618480 and EAR 8416254 to D. H. Lindsley).

References Cited

Akimoto, S. (1954) Thermo-magnetic study of ferromagnetic minerals contained in igneous rocks. Journal of Geomagnetism and Geoelectricity, 6, 1–14.

Andersen, D.J. (1983) The olivine-ilmenite thermometer: New data at 1200 °C. Geological Society of America Abstracts with Programs, 15, 471.

Andersen, D.J., and Lindsley, D.H. (1979) The olivine-ilmenite thermometer. Proceedings of the 10th Lunar and Planetary Science Conference, 493–508.

——— (1981) A Valid Margules formulation for an asymmetric ternary solution: Revision of the olivine-ilmenite thermometer. Geochimica et Cosmochimica Acta, 45, 847–852.

Anderson, A.T. (1968) Oxidation of the LaBlanche Lake titaniferous magnetite deposit, Quebec. Journal of Geology, 76, 528–547.

Barth, T.F.W., and Posnjak, E. (1934) The crystal structure of ilmenite. Zeitschrift für Kristallographie, A88, 265–270.

Berman, R.G., and Brown, T.H. (1984) A thermodynamic model for multi-component melts, with application to the system CaO-Al_2O_3-SiO_2. Geochimica et Cosmochimica Acta, 48, 661–678.

Bleil, U. (1976) An experimental study of the titanomagnetite solid solution series. Pure and Applied Geophysics, 114, 165–175.

Bishop, F.C. (1976) Partitioning of Fe^{2+} and Mg between ilmenite and some ferromagnesium silicates, 137 p. Ph.D. thesis, University of Chicago, Chicago, Illinois.

Buddington, A.F., and Lindsley, D.H. (1964) Iron-titanium oxide minerals and synthetic equivalents. Journal of Petrology, 5, 310–357.

Burton, B.P. (1982) Thermodynamic analysis of the systems $CaCO_3$-$MgCO_3$, αFe_2O_3 and Fe_2O_3-$FeTiO_3$, Ph.D. thesis, State University of New York at Stony Brook.

——— (1987) Recalculation of the Fe_2O_3-$FeTiO_3$ phase diagram. EOS, 68, 296.

Carmichael, I.S.E. (1967) The iron-titanium oxides of salic volcanic rocks and their associated ferromagnesium silicates. Contributions to Mineralogy and Petrology, 14, 36–64.

Chevallier, R., Bolfa, T., and Mathieu, S. (1955) Titanomagnétites et ilménites ferromagnétiques. (1) Etude optique radiocristallographique, chimique. Bulletin de la Société Française de Minéralogie et de Crystallographie, 78, 307–346.

Chou, I.M. (1978) Calibration of oxygen buffers at elevated pressure and temperature using the hydrogen fugacity sensor. American Mineralogist, 63, 650–703.

Darken, L.S., and Gurry, R.W. (1953) Physical chemistry of metals. McGraw-Hill, New York.

de Grave, E., de Setter, J., and Vandenberghe, R. (1975) On the cation distribution in the spinel system yMg_2TiO_4-$(1 - y)MgFe_2O_4$. Applied Physics, 7, 77–84.

El Goresy, A., and Woermann, E. (1977) Opaque minerals as sensitive oxygen barometers and geothermometers in lunar basalts. In D.G. Fraser, Ed., Thermodynamics in geology, p. 249–277. D. Reidel, Boston, Massachusetts.

Frost, B., and Myers, J. (1982) Equilibria between oxides and silicates: An additional constraint on Fe-Ti oxide geothermometry. Geological Society of America Abstracts with Programs, 14, 492.

Hadjigeorgiou, C.H., Grunder, A., and Lindsley, D.H. (1987) Two-oxide, two-feldspar barometry revisited: II. Direct experimental calibration. Geological Society of America Abstracts and Programs, 19, 689.

Hammond, P.L., Tompkins, L.A., Haggerty, S.E., Taylor, L.A., Spencer, K.J., and Lindsley, D.H. (1982) Revised data for coexisting magnetite and ilmenite near 1000 °C, NNO and FMQ buffers. Geological Society of America Abstracts with Programs, 14, 506.

Hill, R.J., Craig, J.R., and Gibbs, G.V. (1979) Systematics of the spinel structure type. Physics and Chemistry of Minerals, 4, 317–339.

Hill, R.L., and Sack, R.O. (1987) Thermodynamic properties of Fe-Mg titaniferous magnetite spinels. Canadian Mineralogist, 25, 443–464.

Jamieson, H.E., and Roedder, P.L. (1984) The distribution of Mg and Fe^{2+} between olivine and spinel at 1300 °C. American Mineralogist, 69, 283–291.

Jensen, S.D., and Shive, P.N. (1973) Cation distribution in sintered titanomagnetites. Journal of Geophysical Research, 78, 8474–8480.

Katsura, T., Wakihara, M., Hara, S.I., and Sugihara, T. (1975) Some thermodynamic properties of spinel solid solutions with the Fe_3O_4 component. Journal of Solid State Chemistry, 14, 107–113.

Katsura, T., Kitayama, K., Aoyagi, R., and Sasajima, S. (1976) High-temperature experiments related to Fe-Ti oxide minerals in volcanic rocks. Kazan (Volcanoes), 1, 31–56 (in Japanese).

Kress, V.C. (1986) Iron-manganese exchange in coexisting garnet and ilmenite. M.S. thesis, State University of New York at Stony Brook.

Lindsley, D.H. (1963) Fe-Ti oxides in rocks as thermometers and oxygen barometers. Carnegie Institution of Washington Year Book 62, 60–65.

——— (1976) The crystal chemistry and structure of oxide minerals as exemplified by the Fe-Ti oxides. In D. Rumble III, Ed., Oxide minerals, L61–L88. Mineralogical Society of America Short Course Notes, Washington, D.C.

——— (1981) Some experiments pertaining to the magnetite-ulvöspinel miscibility gap. American Mineralogist, 66, 759–762.

Lindsley, D.H., and Podpora, C. (1983) Experimental calibration of the equilibrium $Fe_2SiO_4 + 2FeTiO_3 = 2Fe_2TiO_4 + SiO_2$. Geological Society of America Abstracts with Programs, 15, 628.

Lindsley, D.H., and Spencer, K.J. (1982) Fe-Ti oxide geothermometry: Reducing analyses of coexisting Ti-magnetite (Mt) and ilmenite (Ilm). EOS, 63, 471.

Nedler, J.A., and Mead, R. (1965) A simplex method for function minimization. Computer Journal, 7, 308.

Néel, L. (1955) Some theoretical aspects of rock magnetism. Advances in Physics, 4, 191–243.

O'Neill, H.St.C., and Navrotsky, A. (1983) Simple spinels: Crystallographic parameters, cation radii, lattice energies and cation distribution. American Mineralogist, 68, 181–194.

——— (1984) Cation distribution and thermodynamic properties of binary spinel solid solutions. American Mineralogist, 69, 733–753.

O'Reilly, W., and Bannerjee, S.K. (1965) Cation distribution in titanomagnetites $(1 - x)Fe_3O_4$-xFe_2TiO_4. Physics Letters, 17, 237–238.

Pauling, L., and Hendricks, S.B. (1925) The crystal structure of hematite and corundum. Journal of the American Chemical Society, 47, 781–790.

Pinckney, L.R., and Lindsley, D.H. (1976) Effects of magnesium on iron-titanium oxides. Geological Society of America Abstracts with Programs, 8, 1051.

Powell, R., and Powell, M. (1977) Geothermometry and oxygen barometry using coexisting iron-titanium oxides: A reappraisal. Mineralogical Magazine, 41, 257–263.

Price, G.D. (1981) Subsolidus phase relations in the titanomagnetite solid solution series. American Mineralogist, 66, 751–758.

Rumble, D., III. (1970) Thermodynamic analysis of phase equilibria in the system Fe_2TiO_4-Fe_3O_4-TiO_2. Carnegie Institution of Washington Year Book 69, 198–207.

——— (1977) Configurational entropy of magnetite-ulvöspinel$_{ss}$ and hematite-ilmenite$_{ss}$. Carnegie Institution of Washington Year Book 76, 581–584.

Sack, R.O. (1982) Spinels as petrogenetic indicators: Activity-composition relations at low pressures. Contributions to Mineralogy and Petrology, 79, 169–186.

Schmahl, N.G., Frisch, B., and Gartgarter, E. (1960) Zur Kenntnis der Phasenverhaltnisse im System Fe-Ti-O bei 1000°C. Zeitschrift für Anorganische und Allgemeine Chemie, 305, 40–54.

Simons, B., and Woermann, E. (1978) Iron titanium oxides in equilibrium with metallic iron. Contributions to Mineralogy and Petrology, 66, 81–89.

Spencer, K.J., and Lindsley, D.H. (1981) A solution model for coexisting iron-titanium oxides. American Mineralogist, 66, 1189–1201.

Stephenson, A. (1969) The temperature dependent cation distribution in titanomagnetites. Geophysical Journal of the Royal Astronomical Society, 18, 199–210.

Stormer, J.C. (1983) The effects of recalculation on estimates of temperature and oxygen fugacity from analyses of multi-component iron-titanium oxides. American Mineralogist, 68, 586–594.

Taylor, L.A., Williams, R.J., and McCallister, R.H. (1972) Stability relations of ilmenite and ulvöspinel in the Fe-Ti-O system and application of these data to lunar mineral assemblages. Earth and Planetary Science Letters, 16, 282–288.

Taylor, R.W. (1964) Phase equilibria in the system FeO-Fe_2O_3-TiO_2 at 1300 °C. American Mineralogist, 49, 1016–1030.

Taylor, R.W., and Schmalzreid, H. (1964) Free energy of formation of some titanates, silicates, and Mg-aluminate from measurements made with galvanic cells using solid electrolytes. Journal Physics and Chemistry, 68, 2444.

Thompson, J.B., Jr. (1969) Chemical reactions in crystals. American Mineralogist, 54, 341–375.

——— (1970) Chemical reactions in crystals: Corrections and clarification. American Mineralogist, 55, 528–532.

Trestman-Matts, A., Dorris, S.E., Kumarakrishnam, S., and Mason, T.O. (1983) Thermoelectric determination of cation distributions in Fe_3O_4-Fe_2TiO_4. Journal of the American Ceramic Society, 66, 829–834.

Trestman-Matts, A., Dorris, S.E., and Mason, T.O. (1984) Thermoelectric determination of cation distributions in Fe_3O_4-$MgFe_2O_4$. Journal of the American Ceramic Society, 67, 69–74.

Verwey, E.J.W., and Heilmann, E.L. (1947) Physical properties and cation arrangement of oxides with spinel structures: I. Cation arrangement in spinels. Journal of Chemical Physics, 15, 174–187.

Vincent, E.A., Wright, J.B., Chevallier, R., and Mathieu, S. (1957) Heating experiments on some natural titaniferous magnetites. Mineralogical Magazine, 31, 624–655.

Webster, A.H., and Bright, N.F.H. (1961) The system iron-titanium-oxygen at 1200°C and oxygen partial pressures between 1 atmosphere and 2×10^{-14} atmospheres. American Ceramic Society Journal, 44, 110–116.

Wechsler, B.A. (1978) Crystal structure of ilmenite at high temperature. Geological Society of America Abstracts with Programs, 10, 513.

Wechsler, B.A., Lindsley, D.H., and Prewitt, C.T. (1984) Crystal structure and cation distribution in titanomagnetites $(Fe_{3-x}Ti_xO_4)$. American Mineralogist, 69, 754–770.

Wohl, K. (1946) Thermodynamic evaluation of binary and ternary liquid systems. Transactions, American Institute of Chemical Engineering, 42, 215–249.

——— (1953) Thermodynamic evaluation of binary and ternary liquid systems. Chemical Engineering Progress, 49, 218–219.

Wu, C.C., and Mason, T.O. (1981) Thermopower measurement of cation distribution in magnetite. Journal of the American Ceramic Society, 64, 520–522.

Manuscript received July 30, 1987
Manuscript accepted March 21, 1988